LA-UR- 08-4922

*Approved for public release; distribution is unlimited.*

| | |
|---|---|
| *Title:* | Carrier Dynamics in InGaAs with embedded ErAs Nanoislands |
| *Author(s):* | Abul K. Azad, LANL; Rohit P. Prasankumar, LANL; Diyar Talbayev, LANL; Antoinette J. Taylor, LANL; John F. O'Hara, LANL; Richard D. Averitt, LANL; Joshua M.O. Zide, University of Delaware; Hong Lu, UCSB; Arthur C. Gossard, UCSB. |
| *Intended for:* | Applied Physics Letters (Journal) |

Los Alamos
NATIONAL LABORATORY
EST. 1943



Form 836 (7/06)

# Carrier dynamics in InGaAs with embedded ErAs nanoislands

Abul K. Azad*, Rohit P. Prasankumar, Diyar Talbayev, Antoinette Taylor, and John F. O'Hara

*MPA-CINT, Los Alamos National Laboratory, Los Alamos, NM-87544*

Richard D. Averitt

*Department of Physics, Boston University, 590 Commonwealth Avenue, Boston, MA-02215*

Joshua. M. O. Zide

*Electrical and Computer Engineering, University of Delaware, DE-19716*

Hong Lu, Arthur C. Gossard

*Materials Department, University of California, Santa Barbara, CA-93106*

Using time-resolved optical-pump terahertz-probe spectroscopy, we study the ultrafast carrier dynamics in $In_{0.53}Ga_{0.47}As$:ErAs, a potential candidate for 1550 nm based terahertz photoconductive detectors. Material growth is performed by co-depositing ErAs nanoislands with Be-compensated InGaAs on an InP:Fe substrate using molecular beam epitaxy. The material shows a rapid photoconductivity response following optical excitation. Photoexcitation with ~0.5 $\mu J/cm^2$ 800 nm femtosecond laser pulses yields a 3.2 ps carrier lifetime in optical-pump terahertz-probe experiments. We also measure the carrier lifetime using a 1550 nm femtosecond optical pump-probe system, and it is found to agree well with the terahertz measurements. These short lifetimes demonstrate significant potential for implementing terahertz systems using telecommunications based technologies.

*E-mail: aazad@lanl.gov

Despite a growing demand for terahertz (THz) applications, such as imaging, inter-chip communication, short range wireless, and nondestructive spectroscopy [1-3], THz technology still suffers from a serious lack of functional devices, in particular compact and efficient generators and detectors. Photoconductive antennas are prevalent as high-performance THz devices that utilize the optoelectronic response of semiconductors to make THz generation and detection possible with commercially available 800 nm femtosecond lasers. However, the major factor that severely limits their wide applicability is the scarcity of suitable semiconductors having an ultrafast carrier lifetime (~1 ps), low dark current, and simultaneous compatibility with compact powerful ultrafast laser sources. Traditionally, radiation damaged silicon-on-sapphire (RD-SOS) or low temperature grown GaAs (LT-GaAs) is used for photoconductive antennas compatible with 800 nm femtosecond lasers. However, tuning the carrier lifetimes of RD-SOS and LT-GaAs is not exact because of the limitations in fabrication [4-7] and this can result in a degradation of device performance through other parameters (dark current, mobility, etc.). Furthermore, neither semiconductor is amenable to operation with 1550 nm (telecom) lasers, though such lasers offer the advantages of low cost and maintenance, small footprints, excellent noise performance, and naturally low-dispersion pulse delivery via optical fibers. Such lasers are typically frequency doubled to operate THz systems, but this severely reduces the available optical power at the THz devices. In addition, since doubling occurs at the laser, this approach does not take advantage of low-dispersion fiber delivery. To benefit from 1550 nm technology, it is essential to explore alternative semiconductors for THz detection. Some progress has already been made with 1550 nm-based photoconductive switches fabricated on various InGaAs substrates [8-12]. In this Letter, we use optical-pump THz-probe (OPTP) spectroscopy and 1550 nm optical pump-probe measurements to study the carrier dynamics of a promising alternative:

bulk InGaAs:ErAs formed by co-depositing embedded ErAs nanoislands into an InGaAs matrix. We measured carrier relaxation times as short as 3.2 ps, suggesting that this material may be suitable for THz detection antennas that are gated by ultrashort 1550 nm pulses.

The properties of self-assembled ErAs nanoislands embedded in GaAs and InGaAs have been investigated with great interest for ultrafast applications [13-15]. GaAs:ErAs superlattices have high mobility and short (~800 fs) carrier lifetimes [14] and have been shown to produce excellent 800 nm THz detectors [16]. Due to its smaller bandgap, InGaAs:ErAs is suitable for telecom wavelength applications. Optical pump-optical probe measurements at 1550 nm show carrier lifetimes in InGaAs:ErAs superlattices are highly depended on lattice parameters and proper doping [15].

The $In_{0.53}Ga_{0.47}As$:ErAs sample used in this work was grown by molecular beam epitaxy (MBE) on a <100> semi-insulating InP:Fe substrate with a 100 nm InAlAs buffer layer at temperature of 450°C. The InGaAs and ErAs were deposited simultaneously with a growth rate of about 2 μm/hour to form the 2-μm-thick bulk layer of InGaA:ErAs. During growth, the ErAs forms into nanoparticles (traps) in the InGaAs matrix with an average size of ~2 nm. The estimated trap density is about $1\times10^{18}$ $cm^{-3}$. Beryllium compensation is also used to minimize the dark current and results in an n-type free carrier concentration of about $1.3\times10^{15}$ $cm^{-3}$. Figure 1 (inset) shows a schematic cross-section of the sample used for the measurements.

This co-deposited growth offers several potential advantages over the superlattice growth used in previous GaAs:ErAs studies [14, 16]. First, superlattice growth requires numerous interruptions [13], while co-deposited growth does not. Since small layer spacings are desirable for short lifetimes [13, 17], these interruptions (~30 seconds/period) can increase deposition times substantially. The other significant advantage of co-deposited materials is the decreased

average spacing between particles, again desirable for short lifetimes. In a superlattice, the average distance to a particle is $L/2$ (where $L$ is the layer spacing), while the spacing in the co-deposited material scales as $N^{1/3}$, where $N$ is the concentration of ErAs traps.

The OPTP experiment utilizes a 1 kHz regeneratively amplified Ti:Sapphire laser capable of generating 3.2 mJ, 50 fs pulses at 800 nm. Part of the output laser power is used for THz generation and detection using ZnTe crystals via the electro-optic effect [18]. The system generates a ~2.5 THz bandwidth beam that propagates normally through the sample and has a frequency-independent diameter of 4 mm at the focus [14, 19]. The remainder of the optical power passes through a variable attenuator to form a ~10 mm diameter illumination spot at the sample. Measurements were performed at room temperature and in a dry air environment. Optical pump fluences of 0.5, 1.5, 5.0, 10, and 20 $\mu J/cm^2$ were used to excite the sample. The penetration depth of 800 nm light into InGaAs is ~200 nm, so the 2 μm thickness is sufficient to absorb all of the incident pump light.

Figure 1 shows typical time-domain THz pulses following passage through the InGaAs:ErAs sample before (black) and after (blue) optical excitation. Here, the photoexcited THz pulse is recorded 5 ps after pump pulse arrival. Upon optical excitation free carriers generated within the InGaAs attenuate the transmitted THz pulses. Figure 2(a) shows the normalized change of the THz peak electric field $\Delta E(t)/E_0$ as a function of delay between optical pump and THz probe pulses. Here, $\Delta E(t)$ is the time-dependent differential change of the THz peak amplitude and $E_0$ is the peak amplitude of THz pulses without optical excitation. Clearly, the THz transmission decreases as the increasing pump fluence creates more photocarriers. The peak transmission decreased to about 75% of its maximum value when the sample was illuminated with a fluence of 20 $\mu J/cm^2$. The evolution of $\Delta E(t)/E_0$ following photo-excitation shows a characteristic

recovery time that also depends on the pump fluence. $\Delta E(t)/E_0$ approaches zero as the time delay between optical and THz pulse increases, indicating that photocarriers are being trapped by the available ErAs inclusions.

Because of the small penetration depth at 800 nm, we consider the photoexcited layer of InGaAs:ErAs as a highly-conductive film on a semi-infinite insulating substrate. Following photoexcitation, the conductivity of such a film has a time dependence, which can be expressed as [14, 20],

$$\sigma(t) = \frac{1+n}{Z_0 d}\left(\frac{1}{1+\Delta E(t)/E_0} - 1\right) \qquad (1)$$

where $Z_0 = 377\ \Omega$ is the impedance of free space, $n = 3.5$ is the measured refractive index of InGaAs:ErAs at THz frequencies, and $d$ is the optical penetration depth of the pump beam inside the film. The time-dependent photo-induced conductivity is shown in Fig. 2(b). This conductivity is about 3.5 times larger than that of the GaAs:ErAs superlattices [14], due in part to the shorter penetration depth of 800 nm light in InGaAs and the associated higher carrier density. The photo-induced carrier density $N(t)$ is directly related to the conductivity via $\sigma(t) = N(t)\mu e$ where $\mu$ is the mobility and $e$ is the fundamental electronic charge. Hegmann *et al.* measured the fluence-dependent carrier dynamics of RD-SOS and their measured mobility remained almost unchanged [20]. Similarly, given the optical fluence used in this work, it is justifiable to consider the mobility as constant and equal to the measured value of 384 $cm^2/V\text{-}s$ by Hall effect measuments. Figure 2(b) shows the extracted photocarrier density (right scale) from the measured data. Our maximum photocarrier density for 20 $\mu J/cm^2$ is $2\times10^{19}$ $cm^{-3}$, which is consistent with the number of available photons being completely absorbed in ~200 nm. The

photocarrier density shows an exponential decay with time due to carrier trapping in the ErAs nanoislands.

Equation (1) suggests that the transient THz transmission change $\Delta E(t)$ is proportional to the number of free photocarriers. Figure 3(a) shows the normalized $|\Delta E(t)|$ as a function of pump delay for all fluences. The transient THz change $\Delta E(t)$ can be fit (solid lines) by the convolution of a 1.3-ps Gaussian experimental response (the THz pulse duration) and a bi-exponential decay function [21]. The bi-exponential represents two characteristic decay times involved in the relaxation process. The fast decay component $\tau_1$ near $t = 0$ varies with the pump fluence and represents rapid photocarrier capture by the ErAs traps. Fig 3(b) shows the corresponding fitting values of the fast decay time $\tau_1$ as a function of the pump fluence. The shortest $\tau_1 = 3.2$ ps was obtained when the optical fluence was 0.5 $\mu J/cm^2$. However, $\tau_1$ increases with pump fluence. This is caused by trap saturation occurring when the density of photocarriers exceeds the density of available traps ($\sim 1\times10^{18}$ $cm^{-3}$). The longer decay component $\tau_2$ is ~75 ps and is independent of the pump fluence. Though the longer decay is still under investigation, it may be due to trapping at growth defects, shallow defect states near the ErAs particles, or Be-based complexes.

Since InGaAs:ErAs is an appropriate material for ultrafast switches at telecom wavelengths we also measured the photocarrier lifetime using 1550 nm optical pump-probe reflection measurements. We used an IMRA brand femtosecond fiber laser system (BX-60) that generates ~60 fs pulses with an average output power of 80 mW. Most of the power is used to pump the sample and the remainder is used to probe the reflection change ($\Delta R$), which is proportional to the generated photocarrier density [21]. We performed the measurements for two different optical fluences, 20 $nJ/cm^2$ (blue curve) and 5 $nJ/cm^2$ (red curve), as shown in Fig. 4. The

normalized change in reflectivity ($\Delta R/R$) is approximately $10^{-5}$, which translates into an estimated photocarrier density of ~$10^{14}$ $cm^{-3}$, much lower than the available trap density. We note that the penetration depth of 1550 nm light is ~2 μm in InGaAs:ErAs. These data can be modeled using a 100 fs Gaussian response function together with a single exponential having a characteristic decay time of 2.6 ps. There is no apparent difference in decay times for the 20 and 5 $nJ/cm^2$ excitations. These lifetimes are consistent with our low fluence 800 nm OPTP measurements. Again, this indicates that the photocarrier relaxation process is dominated by the ErAs trapping time under low fluence excitation (< 0.5 $\mu J/cm^2$). Though this InGaAs:ErAs sample has a longer carrier lifetime than previous GaAs:ErAs superlattice samples [14] there is still some degree of lifetime reduction available by increasing the density of ErAs traps.

In conclusion, we have measured the carrier relaxation dynamics of co-deposited InGaAs:ErAs. Our 800 nm optical-pump THz-probe measurements show carrier lifetimes of ~3 ps when excited with low fluence. This is confirmed by optical pump-probe measurements using a 1550 nm pulsed fiber laser. This material has a high potential for use in photoconductive THz detectors compatible with compact telecommunication-wavelength lasers. Our measurements also provide an estimate of optical fluence limitations and their relation to maximizing THz bandwidth.

This work was performed in part, at the Center for Integrated Nanotechnologies, a U. S. Department of Energy, Office of Basic Energy Sciences Nanoscale Science Research Center jointly operated by Los Alamos and Sandia National Laboratories. Los Alamos National Laboratory, an affirmative action equal opportunity employer, is operated by Los Alamos National Security, LLC, for the National Nuclear Security Administration of the U. S. Department of Energy under contract DE-AC52-06NA25396.

**References:**


1. Sensing with Terahertz Radiation, edited by D. M. Mittleman (Springer Verlag, Berlin, 2003).
2. J. F. O'Hara and D. Grischkowsky, Opt. Lett. **27**, 1070 (2002).
3. A. K. Azad, J. Han, and W. Zhang, Appl. Phys. Lett. **88**, 021103 (2006).
4. S. Gupta and J. F. Whitaker, IEEE J. Quantum Electron, 28, 2464 (1992).
5. F. E. Donay, D. Grischkowsky, and C. –C. Chi, Appl. Phys. Lett, **50**, 460 (1987).
6. D. C. Look, J. Appl. Phys. **70**, 3148 (1991).
7. M. C. Beard, G. M. Turner, and C. A. Schmuttenmaer, J. Appl. Phys. **90**, 5915 (2001).
8. A. Takazato, M. Kamakura, T. Matsui, J. Kitagawa, and Y. Kadoya, Appl. Phys. Lett. **90**, 101119 (2007).
9. A. Takazato, M. Kamakura, T. Matsui, J. Kitagawa, and Y. Kadoya, Appl. Phys. Lett. **91**, 011102 (2007).
10. M. Suzuki and M. Tonouchi, Appl. Phys. Lett. **86**, 051104 (2005).
11. M. Suzuki and M. Tonouchi, Appl. Phys. Lett. **86**, 163504 (2005).
12. L. Meignien, J. Mangeney, P. Crozat, L. Duvillaret, and M. Hanna, Appl. Phys. Lett. **92**, 131103 (2008).
13. C. Kadow, S. B. Fleischer, J. P. Ibbetson, J. E. Bowers, A. C. Gossard, J. W. Dong, and C. J. Palmstrom, Appl. Phys. Lett. **75**, 3548 (1999).
14. R. P. Prasankumar, A. Scopatz, D. J. Hilton, A. J. Taylor, and R. D. Averitt, Appl. Phys. Lett. **86**, 201107 (2005).
15. D. C. Driscoll, M. P. Hanson, A. C. Gossard, and E. R. Brown, Appl. Phys. Lett. **86**, 051908 (2005).

16. J. F. O'Hara, J. M. O. Zide, A. C. Gossard, A. J. Taylor, and R. D. Averitt, Appl. Phys. Lett. **88**, 251119 (2006).

17. H.-T. Chen, W. J. Padilla, J. M. O. Zide, S. R. Bank, A. C. Gossard, A. J. Taylor, and R. D. Averitt, Opt. Lett. **32**, 1620 (2007).

18. Q. Wu, M. Litz, and X.-C. Zhang, Appl. Phys. Lett. **68**, 2924 (1996).

19. H. –T. Chen, J. F. O'Hara, A. K. Azad, A. J. Taylor, R. D. Averitt, D. B. Shrekenhamer and W. J. Padilla, Nat. Photon. **2**, 295(2008),

20. K. P. H. Lui and F. A. Hegmann, Appl. Phys. Lett. **78**, 3478 (2001).

21. F. E. Doany and D, Grischkowsky, Appl. Phys. Lett. **52**, 36 (1988).

## FIGURE CAPTIONS:

Fig. 1: Time-dependent THz pulses transmitted through InGaAs:ErAs samples. The black and the blue curves represent the transmitted THz pulses before and after optical excitation (~ 5 $\mu J/cm^2$), respectively. Amplitudes are normalized to the unexcited pulse amplitude maximum. The inset shows a cross-sectional view of the sample.

Fig. 2: Optical-pump THz-probe measurements at various pump fluence with 800 nm pump. (a) Pump-induced transmission change normalized to the unexcited THz amplitude maximum, $\Delta E(t)/E(0)$, as a function of pump delay. (b) Photo-induced conductivity $\sigma(t)$ (left $y$-axis) and carrier density $N(t)$ (right $y$-axis) vs time delay. Pump fluence 0.5, 1.5, 5, 10, and 20 $\mu J/cm^2$ are represented by black, blue, red, cyan, and purple colors, respectively.

Fig. 3: (a) Transmission change $|\Delta E(t)|$ normalized to unity at different fluences (same color scheme as in Fig. 2). Dots show measured data while smooth curves show the bi-exponential fit. (b) Fluence dependent carrier lifetimes.

Fig. 4: Transient reflectivity changes ($|\Delta R|$) measured in 1550 nm optical pump-probe experiments as a function of pump delay. For comparison $|\Delta R|$ is normalized to unity.

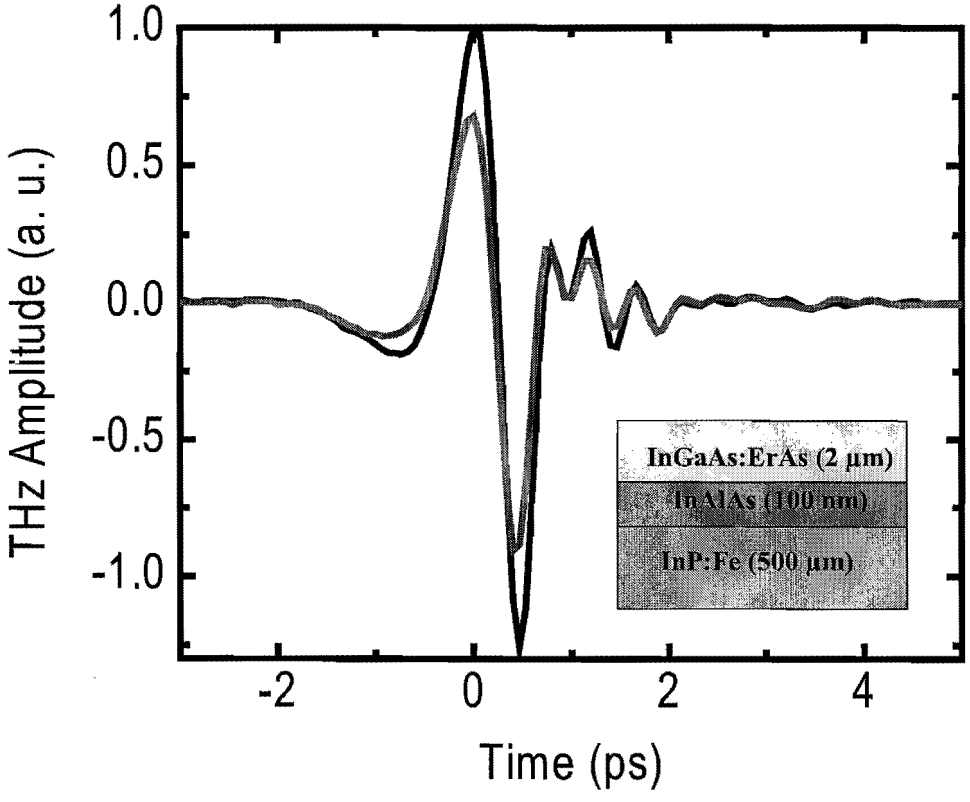
1.0
0.5
0.0
-0.5
-1.0
THz Amplitude (a. u.)
-2
0
2
4
Time (ps)
InGaAs:ErAs (2 µm)
InAlAs (100 nm)
InP:Fe (500 µm)

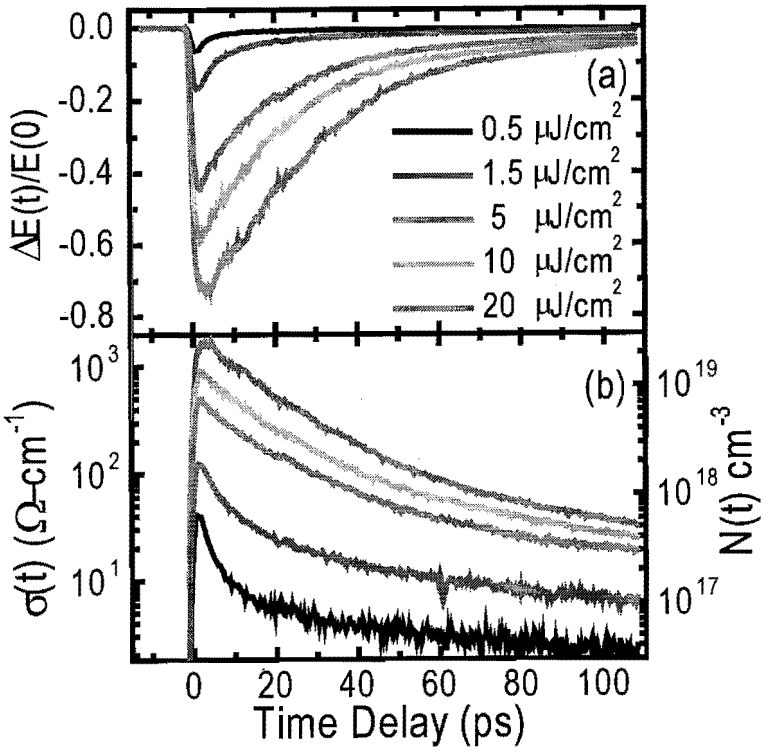
0.0
-0.2
-0.4
-0.6
-0.8
ΔE(t)/E(0)
(a)
0.5 μJ/cm2
1.5 μJ/cm2
5 μJ/cm2
10 μJ/cm2
20 μJ/cm2
10^3
10^2
10^1
σ(t) (Ω-cm)^-1
(b)
10^19
10^18
10^17
N(t) cm^-3
0
20
40
60
80
100
Time Delay (ps)

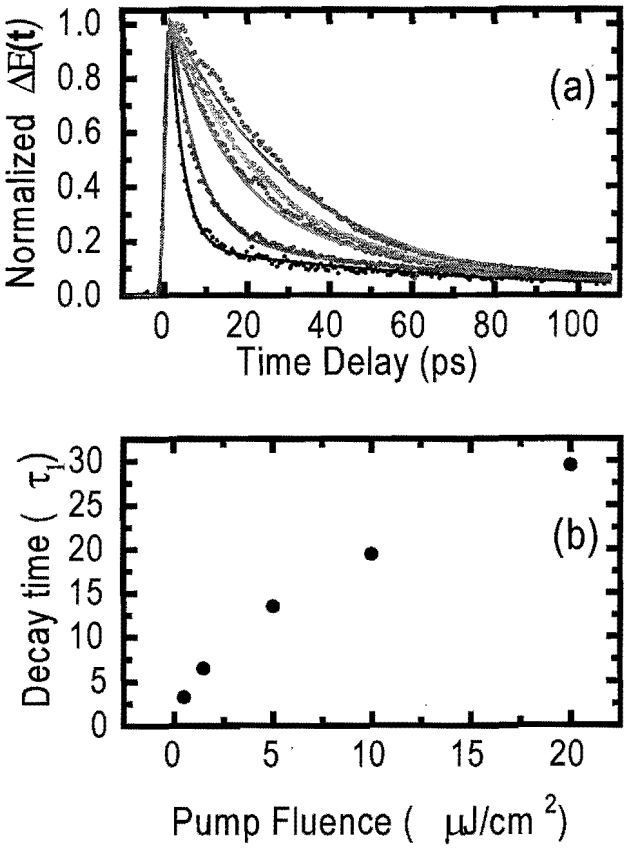
Normalized ΔE(t)
1.0
0.8
0.6
0.4
0.2
0.0
(a)
0
20
40
60
80
100
Time Delay (ps)
Decay time ( τ1)
30
25
20
15
10
5
0
(b)
0
5
10
15
20
Pump Fluence ( μJ/cm 2)

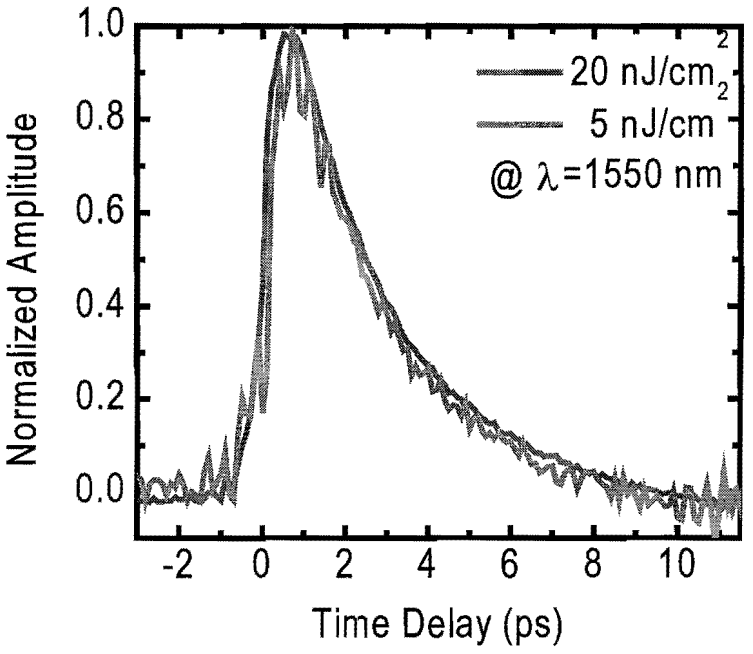
1.0
0.8
0.6
0.4
0.2
0.0
Normalized Amplitude
-2
0
2
4
6
8
10
Time Delay (ps)
20 nJ/cm2
5 nJ/cm2
@ λ=1550 nm